Bipolar Plasma Membrane Distribution of Phosphoinositides and Their Requirement for Auxin-Mediated Cell Polarity and Patterning in *Arabidopsis*[W]

Ricardo Tejos,[a,b,1] **Michael Sauer,**[a,b,2] **Steffen Vanneste,**[a,b] **Miriam Palacios-Gomez,**[c] **Hongjiang Li,**[c]
Mareike Heilmann,[d] **Ringo van Wijk,**[e] **Joop E.M. Vermeer,**[e,3] **Ingo Heilmann,**[d] **Teun Munnik,**[e] **and Jiří Friml**[a,b,c,4]

[a] Department of Plant Systems Biology, VIB, 9052 Ghent, Belgium
[b] Department of Plant Biotechnology and Bioinformatics, Ghent University, 9052 Ghent, Belgium
[c] Institute of Science and Technology Austria, 3400 Klosterneuburg, Austria
[d] Department of Cellular Biochemistry, Martin-Luther-University Halle-Wittenberg, 06120 Halle (Saale), Germany
[e] Swammerdam Institute for Life Sciences, Section Plant Physiology, University of Amsterdam, 1098 XH Amsterdam, The Netherlands

Cell polarity manifested by asymmetric distribution of cargoes, such as receptors and transporters, within the plasma membrane (PM) is crucial for essential functions in multicellular organisms. In plants, cell polarity (re)establishment is intimately linked to patterning processes. Despite the importance of cell polarity, its underlying mechanisms are still largely unknown, including the definition and distinctiveness of the polar domains within the PM. Here, we show in *Arabidopsis thaliana* that the signaling membrane components, the phosphoinositides phosphatidylinositol 4-phosphate (PtdIns4P) and phosphatidylinositol 4,5-bisphosphate [PtdIns(4,5)P_2] as well as PtdIns4P 5-kinases mediating their interconversion, are specifically enriched at apical and basal polar plasma membrane domains. The PtdIns4P 5-kinases PIP5K1 and PIP5K2 are redundantly required for polar localization of specifically apical and basal cargoes, such as PIN-FORMED transporters for the plant hormone auxin. As a consequence of the polarity defects, instructive auxin gradients as well as embryonic and postembryonic patterning are severely compromised. Furthermore, auxin itself regulates PIP5K transcription and PtdIns4P and PtdIns(4,5)P_2 levels, in particular their association with polar PM domains. Our results provide insight into the polar domain–delineating mechanisms in plant cells that depend on apical and basal distribution of membrane lipids and are essential for embryonic and postembryonic patterning.

INTRODUCTION

Multicellular organisms rely on their capacity to break cellular symmetry and generate new axes of polarity to build their complex structures. Cell polarity, understood as the existence of two opposite structural or functional poles, is the initial characteristic necessary for an organism to generate asymmetries at a large scale (Li and Bowerman, 2010). The molecules and factors that determine and maintain cell polarity are well characterized in mammalian cells, including the interplay among the so-called "polarity complexes," which are also partially conserved in yeast (Assémat et al., 2008; Thompson, 2013). In plants, cell polarity is considered to be crucial during both embryonic and postembryonic development and during responses to the environment (Dettmer and Friml, 2011). However, the general notion of polarity complexes is absent, and thus the mechanisms found in other eukaryotes cannot be directly extrapolated to plants (Geldner, 2009).

One of the manifestations of cell polarity is the asymmetric distribution of proteins and lipids at the plasma membrane (PM). Plant cells have reached a complex structural asymmetry by the generation of four different PM polar domains in a single cell type, such as the root epidermis (Dettmer and Friml, 2011). The best studied polar cargoes in plants are the PIN-FORMED (PIN) transporters, which are essential for directional movement of the hormone auxin and its patterning signal; hence, their polar localization is a fundamental feature of their function (Petrásek et al., 2006; Wisniewska et al., 2006). Initial insights into the processes and factors determining PIN polarity have highlighted the role of clathrin-mediated endocytosis (Kitakura et al., 2011) and constitutive recycling and trafficking for PIN polarity maintenance (Kleine-Vehn et al., 2011; Tanaka et al., 2013) and the involvement of PIN phosphorylation in their sorting to apical versus basal polar domains (Friml et al., 2004; Michniewicz et al., 2007). Additionally, auxin itself has been shown to regulate the capacity of its own transport through the inhibition of clathrin-mediated endocytosis and PIN internalization (Paciorek et al., 2005; Robert et al., 2010), to regulate PIN protein vacuolar trafficking (Abas et al., 2006; Baster et al., 2013), and to dynamically change PIN polarity in different developmental contexts (Benková

---

et al., 2003; Heisler et al., 2005; Sauer et al., 2006a; Scarpella et al., 2006; Ikeda et al., 2009; Balla et al., 2011). To date, it is not entirely clear how auxin modulates PIN polarity: while the underlying mechanism requires at least to some extent nuclear TRANSPORT INHIBITOR RESPONSE1 (TIR1)–, auxin/indole-3-acetic acid (Aux/IAA)–, and auxin response factor (ARF)–mediated auxin-dependent transcription (Chapman and Estelle, 2009), the mechanism does not involve any known regulator of PIN trafficking and polarity (Sauer et al., 2006a). Thus, which processes downstream of auxin signaling mediate dynamic cell polarity changes and how they are integrated with known trafficking and polarity mechanisms are still unknown, along with many other components that organize the polarity machinery in plant cells.

Phosphoinositides (PIs), the phosphorylated derivatives of the membrane phospholipid phosphatidylinositol, are functionally important lipid constituents of all cellular membranes. PIs function as scaffolding signals to recruit protein effectors to different intracellular compartments as well as signaling molecules involved in numerous cellular processes (Di Paolo and De Camilli, 2006; Ischebeck et al., 2010; Munnik and Nielsen, 2011). In animal systems, polarized cell types use PI asymmetry at their PM as a way to establish and maintain their cellular and tissue polar constitution (Gassama-Diagne et al., 2006; Martin-Belmonte et al., 2007), highlighting a critical function of PI compartmentalization in generating spatial cues important for polarity generation. In plants, there is extensive evidence for the role of PIs and PI-derived signaling in polar tip growth. In particular, phosphatidylinositol 4-phosphate (PtdIns4P) and phosphatidylinositol 4,5-bisphosphate [PtdIns(4,5)P_2] seem to be key metabolites, since they localize specifically to a tip-focused PM domain of growing root hairs (Braun et al., 1999; van Leeuwen et al., 2007; Stenzel et al., 2008; Thole et al., 2008; Vermeer et al., 2009) and pollen tubes (Kost et al., 1999; Dowd et al., 2006; Helling et al., 2006; Ischebeck et al., 2008), expanding cell plates during cytokinesis (van Leeuwen et al., 2007; Vermeer et al., 2009), and are required for the proper development of these highly polarized structures. The conversion of PtdIns4P into PtdIns(4,5)P_2 is catalyzed by phosphatidylinositol 4-phosphate 5-kinases (PI4P 5-kinases) (Mueller-Roeber and Pical, 2002). PtdIns(4,5)P_2 as well as the PI-derived second messengers phosphatidic acid (PtdOH) and inositol 1,4,5-trisphosphate were shown to modulate the trafficking or polarity of PIN proteins (Li and Xue, 2007; Zhang et al., 2011; Mei et al., 2012; Ischebeck and Werner et al., 2013), pointing to a pivotal role of PIs in cell polarity and auxin transport–dependent development.

Here, we show that the main two ubiquitously expressed PI4P 5-kinases, PIP5K1 and PIP5K2 (Stenzel et al., 2008), their substrate PtdIns4P, and their product PtdIns(4,5)P_2 are all specifically enriched at apical and basal PM polar domains in root cells. *PIP5K1* and *PIP5K2* are redundantly required for PIN polarity, auxin distribution, and embryonic as well as postembryonic tissue patterning. In addition, auxin regulates the transcription of *PIP5K1* and *PIP5K2* and modulates PtdIns(4,5)P_2 levels, including PI contents at the PM. Our results suggest a role for PIs in defining polar domains and polarity in plant cells and identify an auxin regulatory input into this mechanism.

RESULTS

PtdIns4P and PtdIns(4,5)P_2 Have Bipolar Localization in *Arabidopsis thaliana* Root Cells

To gain insight into the localization of the two important PIs, PtdIns4P and PtdIns(4,5)P_2, we used two genetically encoded fluorescent reporters that are based on the specific binding of two distinct pleckstrin homology (PH) domains from mammalian proteins: the PH domain of the phospholipase C δ1 (YFP-PH$_{PLC\delta1}$) that specifically binds PtdIns(4,5)P_2 (van Leeuwen et al., 2007) and the PH domain of the human protein FAPP1 (YFP-PH$_{FAPP1}$) that specifically binds PtdIns4P (Vermeer et al., 2009). We analyzed *Arabidopsis* plants expressing both markers under the control of two different constitutive promoters showing different expression levels: the strong cauliflower mosaic virus 35S promoter (van Leeuwen et al., 2007; Vermeer et al., 2009) (Figures 1A and 1C; Supplemental Figure 1) and the *Arabidopsis UBIQUITIN10* (*UBQ10*) promoter (Figures 1B and 1D; Supplemental Figure 2). Using these different reporter lines, we consistently detected an enrichment of fluorescence signals to the apical and basal sides of root epidermal cells (Figures 1A and 1B; Supplemental Figures 1 and 2), cortex, and procambial cells (Supplemental Figure 2). Importantly, the bipolar localization patterns manifested in cells expressing only low levels of the reporters, as indicated by low fluorescence intensities (Figures 1B and 1D), in which perturbation of cellular function by the reporter expression was minimal. By using antibodies raised against liposomes enriched in PtdIns4P or PtdIns(4,5)P_2, we also detected weak signals distributed in a bipolar pattern enhanced at the apical and basal cell sides (Supplemental Figure 3). The antibodies used might also cross-react in vitro with other lipids, such as phosphatidylinositol 3,4-bisphosphate or phosphatidylinositol-3,4,5-trisphosphate, but from our current understanding these PI isomers are not produced in plant cells (Heilmann, 2009; Munnik and Testerink, 2009; Munnik and Nielsen, 2011). Thus, visualization of PIs with established markers, supported by immunolocalization, suggests enrichment of PtdIns4P and PtdIns(4,5)P_2 at apical and basal PM domains.

PIP5K1 and PIP5K2 Have Bipolar Localization throughout Plant Development

As PIs can be enriched at certain membranes by the local metabolism of kinases, phosphatases, and phospholipases, we tested the cellular distribution of the PI4P 5-kinases that phosphorylate PtdIns4P to PtdIns(4,5)P_2. In plants, the function of PI4P 5-kinases is required for various trafficking-dependent processes, among others for polar tip growth (Ischebeck et al., 2008, 2011; Kusano et al., 2008; Sousa et al., 2008; Stenzel et al., 2008; Zhao et al., 2010) and PIN-mediated root gravitropism (Mei et al., 2012; Ischebeck and Werner et al., 2013). The *Arabidopsis* genome contains genes for 11 isoforms of PI4P 5-kinases, of which *PIP5K4* to *PIP5K6*, *PIP5K10*, and *PIP5K11* are pollen expressed (Ischebeck et al., 2008, 2011; Sousa et al., 2008; Zhao et al., 2010) and *PIP5K3* is exclusively expressed in trichoblast and root hairs (Kusano et al., 2008; Stenzel et al., 2008). *PIP5K9* is ubiquitously expressed, localizes to the nucleus and PM, and is involved in the regulation of sugar-mediated root growth (Lou et al., 2007). *PIP5K1* and *PIP5K2*
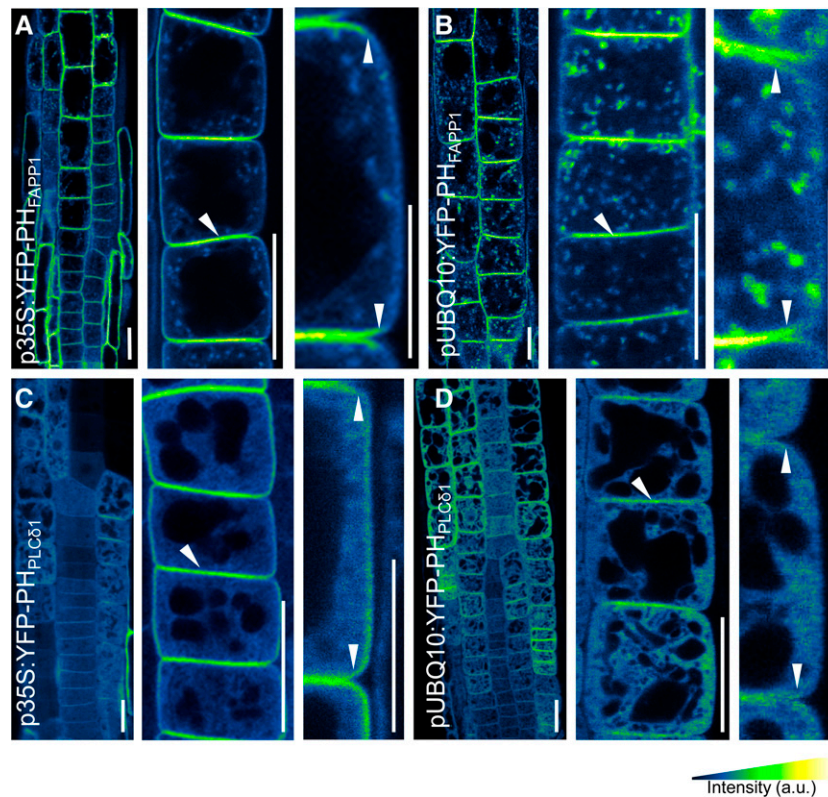
Figure 1. PIs Are Polarly Localized in Root Cells.

Root epidermal cells of 4-d-old seedlings harboring PI biosensors were imaged using confocal microscopy. Images are displayed using a color gradient to indicate low (black/dark blue) to high (yellow) fluorescence intensity.

(A) and **(B)** PtdIns4P biosensor YFP-PH$_{FAPP1}$, driven by the cauliflower mosaic virus promoter 35S (p35S) **(A)** and the *UBQ10* promoter (pUBQ10) **(B)**.

(C) and **(D)** PtdIns(4,5)P$_2$ biosensor YFP-PH$_{PLC\delta1}$, driven by the p35S **(C)** and pUBQ10 **(D)** promoters.

Arrowheads highlight the polar localization of the markers. Bars in the left and middle images in each panel = 20 μm; bars in the right images in each panel = 10 μm.

were chosen for our study because the isoforms they encode have been shown to be the most active among the ubiquitously expressed PI4P 5-kinases (Stenzel et al., 2008) and likely make a major contribution to cellular PtdIns(4,5)P$_2$ formation. Furthermore, PIP5K2 regulates lateral root density and PIN trafficking upon gravistimulation by modulating PIN cycling (Mei et al., 2012), making PIP5K2 a likely candidate for locally producing PtdIns(4,5)P$_2$ in root cells. Because *PIP5K2* and *PIP5K1* form a closely related homologous gene pair (Mueller-Roeber and Pical, 2002; Stenzel et al., 2012) and partially overlap in expression throughout the plant (Supplemental Figure 4), these isoforms were targeted for further characterization.

To visualize the subcellular localization of PIP5K1 and PIP5K2, functional translational fusions with yellow fluorescent protein (YFP) were generated (Ischebeck and Werner et al., 2013; Supplemental Figure 5). The expression patterns of the fusion proteins in the root apical meristem expressed under the control of their respective native promoters resembled those found using the transcriptional reporters (compare Figures 2A and 2B with Supplemental Figure 4) and those reported previously (Elge et al., 2001; Mei et al., 2012; Ischebeck and Werner et al., 2013). YFP-PIP5K1 and YFP-PIP5K2 localized in the cytosol and prominently in nuclei and at the PM

(Figures 2A and 2B). The nuclear localization hints at a possible function of PI4P 5-kinases during *Arabidopsis* development, possibly modulating DNA biosynthesis, transcription, or cell cycle control, as has been found for animal cells (Dieck et al., 2012). Importantly, YFP-PIP5K1 and YFP-PIP5K2 were found to be apical–basal localized in the PM of root procambial and epidermal cells, respectively (Figures 2A and 2B). Similar localization patterns were found for YFP-PIP5K1 in all cell types in the root apical meristem when expressed under the control of a weak constitutive promoter (−2000 bp upstream of the ATG codon of *DNAJc17*) (Figure 2C). The bipolar localization of PIP5K1 and PIP5K2 was further supported by their colocalization with known apical and basal cargoes such as PIN1 and PIN2 in stele and epidermis, respectively (Supplemental Figure 6). Quantification of the fluorescent signal, by evaluating the apical–basal versus lateral fluorescence ratio (polarity index), confirmed the enrichment in polar apical and basal PM domains for PtdIns4P, PtdIns(4,5)P$_2$, and the two PI4P 5-kinases in different cell types (Figure 3; Supplemental Figure 7).

We also tested the localization of PIP5K1 in other developmental contexts, as suggested by their expression patterns (Supplemental Figure 4), using YFP-PIP5K1 expression controlled by the promoter of *DNAJc17* to overcome the weak expression

levels of the constructs under the control of the native promoter. PIP5K1 localized polarly at the PM in the embryo (Figure 2D) and during lateral root primordium development (Figure 2E), where nuclear localization was also observed (Figure 2E). Together, these results reveal that the apical and basal PM of different root cell types is enriched in PtdIns4P and PtdIns(4,5)P$_2$ compared with the lateral PM of the same cells. This PI enrichment coincides with the localization of the PI4P 5-kinases, PIP5K1 and

PIP5K2, suggesting that these enzymes are important for the specification of PI-enriched apical and basal polar domains.

Mutants Lacking PIP5K1 and PIP5K2 Have Defects in Auxin Distribution and Auxin-Dependent Development

To gain insight into the function of *PIP5K1* and *PIP5K2*, we isolated representative knockout mutants in both genes (Supplemental
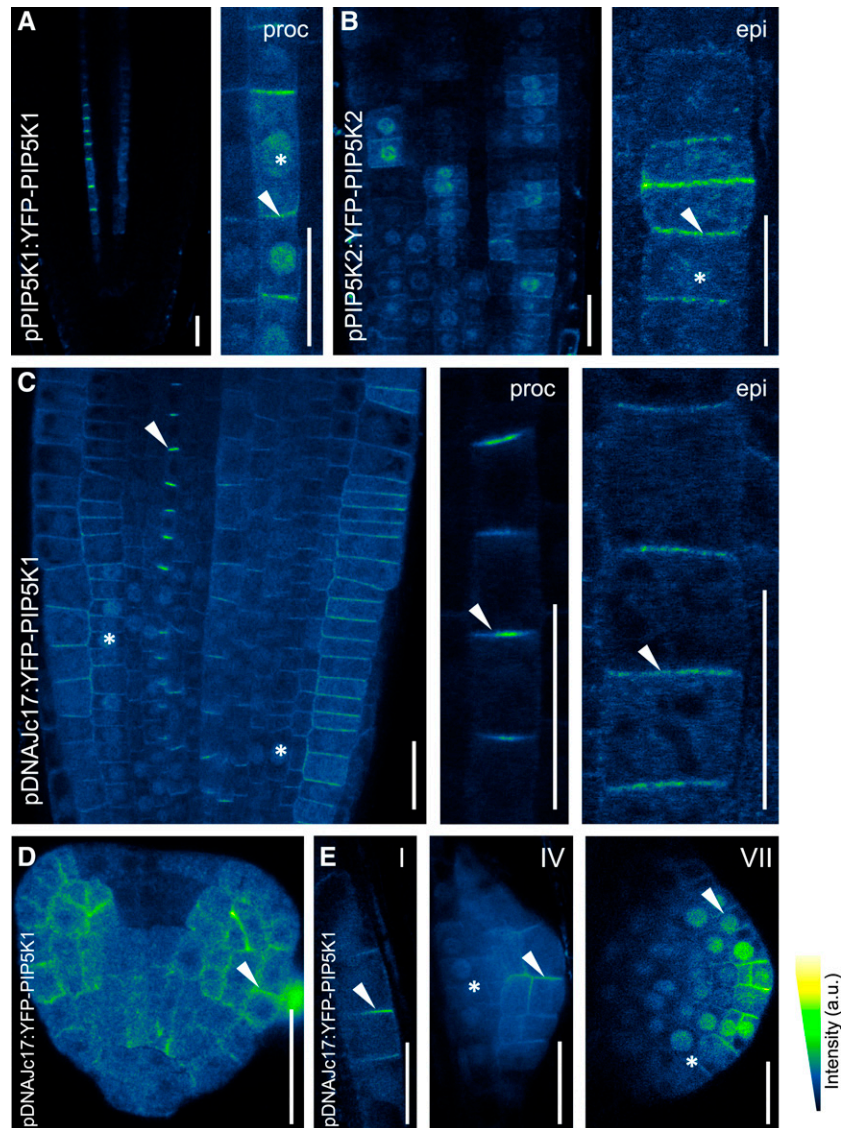

Figure 2. PIP5K1 and PIP5K2 Expression and Subcellular Localization.

(A) and **(B)** PIP5K1 **(A)** and PIP5K2 **(B)** expression under the control of their respective native promoters imaged in 4-d-old root tip seedlings using confocal microscopy. YFP-PIP5K1 is predominantly expressed in procambial cells and YFP-PIP5K2 in epidermal cells. Both PIP5Ks are localized to apical–basal PM (arrowheads), apart from a strong nuclear localization (asterisks).

(C) Live imaging of 4-d-old seedlings using confocal microscopy of YFP-PIP5K1 in the apical root meristem expressed under the control of the weak constitutive promoter of *Arabidopsis DNAJc17* (AT5G23590). YFP-PIP5K1 is asymmetrically localized to the apical and basal cell sides of procambial (proc; middle panel) and epidermal (epi; right panel) cells.

(D) and **(E)** Asymmetrical localization of YFP-PIP5K1 in heart embryo cells **(D)** and at different developmental stages of lateral root primordia in 10-d-old seedlings **(E)**. Lateral root primordia stages indicated in the top right corners are as described by Malamy and Benfey (1997).

Arrowheads highlight polar localization, and asterisks indicate nuclear localization. Bars = 20 μm.
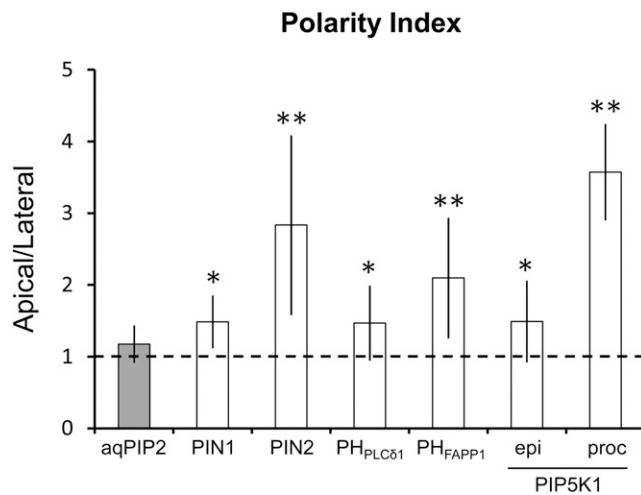
Polarity Index

Figure 3. PI and PIP5K Polarity Indexes.

Apical/basal-to-lateral fluorescence ratio (polarity index) of PI biosensors expressed under the control of the 35S promoter and PIP5K1 proteins in root epidermis (epi) and procambial (proc) cells expressed under the control of the *DNAJc17* promoter. As an apolar marker, we measured the aquaporin PLASMA MEMBRANE INTRINSIC PROTEIN2 (aqPIP2)-GFP in root epidermis cells, and we used PIN1-GFP and PIN2-GFP as polar markers in stele and epidermal root cells, respectively. The dotted line indicates a 1:1 ratio corresponding to a theoretical symmetrically localized PM protein. Root cells of seedlings 4 d after germination were quantified. Bars show means ± SD. A two-tailed Student's *t* test compared data with aqPIP2-GFP values. *P < 0.05, **P < 0.005. n ˃ 20 cells corresponding to roots imaged under comparable conditions.

Figure 8A), and because of their close homology, we also generated double mutants. Each single mutant displayed significantly shorter primary roots and lower lateral root density than the wild type (Supplemental Figure 8B). In the double mutant, root length was even shorter than in the single mutants, and fewer lateral roots were formed (Supplemental Figure 8B). Due to the inability of the double mutant to flower and generate seeds (Supplemental Figures 8C and 8E), the double mutants needed to be reidentified from the segregating offspring of self-pollinated *pip5k1$^{-/-}$ pip5k2$^{+/-}$* parents. The double mutant phenotype in seedlings segregated at a proportion below the expected 25% (χ^2 = 44,610, P < 0.0001; Supplemental Table 1), suggesting a defect in embryogenesis. Therefore, we analyzed the embryo morphology in siliques of *pip5k1$^{-/-}$ pip5k2$^{+/-}$* plants. In the embryos from the segregating population, 12% (n = 121) showed strong deviations from the normal developmental pattern (Figures 4A and 4B; Supplemental Table 1). As early as the two-celled embryo, abnormal patterns of cell division could be observed (Figure 4B). Later in development, defects became more pronounced, resulting in embryos with severe patterning defects and an ill-defined apical-to-basal boundary (Figure 4B).

As the observed mutant aberrations were strongly reminiscent of defects in auxin distribution and signaling, we introduced the synthetic auxin-response reporter, DR5 (Ulmasov et al., 1997), to indirectly visualize the auxin-response distribution. During embryogenesis, DR5 maxima are typically observed near the future

root pole, in the uppermost suspensor cell and in the hypophysis, and, later on, in the incipient cotyledons and provascular strands (Figure 4C; Benková et al., 2003; Friml et al., 2003). By contrast, mutant *pip5k1$^{-/-}$ pip5k2$^{-/-}$* embryos displayed only weak DR5rev:GFP (for green fluorescent protein) activity throughout embryogenesis and often failed to establish localized auxin maxima (Figure 4D). In a proportion of *pip5k1$^{-/-}$ pip5k2$^{-/-}$* mutant embryos (16%, n = 30), ectopic DR5 maxima were seen in patches in the protodermal layer (Figure 4D), with overall high signal in the whole suspensor (6.6%, n = 30; Figure 4D).

Because no aberrant embryos could be found at later stages, development seemed arrested prior to the globular stage in the strongly affected embryos. Nevertheless, 5% (n = 230) of the *pip5k1$^{-/-}$ pip5k2$^{-/-}$* double mutant embryos escaped lethality and established seedlings with defective cotyledons (Supplemental Figures 8F to 8I). Double mutant cotyledons also showed severe defects in vascular development, manifesting in disjointed vascular strands and the formation of so-called vascular islands, completely disconnected vascular fragments (Figure 4E). Similar vascular defects were also observed in primary leaves of 7-d-old and adult *pip5k1$^{-/-}$ pip5k2$^{-/-}$* plants (Supplemental Table 2 and Supplemental Figures 8J and 8K). Postembryonically, most of the *pip5k1$^{-/-}$ pip5k2$^{-/-}$* double mutants displayed dramatically reduced dimensions of the root apical meristem (Figure 4F) and showed decreased DR5:GUS (for β-glucuronidase) activity in the root tips (Figure 4G), although the overall DR5 signal distribution pattern looked normal. In summary, this reverse genetic analysis revealed that *PIP5K1* and *PIP5K2* are essential for asymmetric auxin distribution as well as for embryonic apical–basal patterning, aerial and root-derived organogenesis, leaf venation, and root meristem activity and growth, processes that all depend on asymmetric auxin distribution (Vanneste and Friml, 2009) and typically involve coordinated cell polarization events (Dettmer and Friml, 2011).

Mutants Lacking PIP5K1 and PIP5K2 Have Defects in PIN Polarity

To test whether *PIP5K1* and *PIP5K2* are required for the distribution of apical and basal polar cargoes, we examined the polar distribution of PINs in different developmental contexts in wild-type controls and *pip5k1$^{-/-}$ pip5k2$^{-/-}$* double mutants. During wild-type embryogenesis, PIN1 localization was apical in the protodermal layer, gradually pointing toward the incipient cotyledons, whereas it was basal in the provascular tissues, directing the auxin fluxes toward the forming root pole (Figure 5A), and these patterns are consistent with previous reports (Friml et al., 2003). By contrast, in *pip5k1$^{-/-}$ pip5k2$^{-/-}$* embryos, these polar distribution patterns were severely compromised: PIN1 displayed apolar or uncoordinated, random polar distribution (Figure 5A). Moreover, in the wild type, the PIN1 expression was restricted to the apical cell lineage (proembryo), whereas in *pip5k1$^{-/-}$ pip5k2$^{-/-}$* embryos, it occurred also in suspensor cells (Figure 5B), confirming an apical–basal specification defect. Postembryonically, in wild-type root meristems, PIN2 localizes apically (shootward) in epidermis cells and displays a basal (rootward) localization in young cortex cells, which gradually shifts to apical when cortex cells start to elongate and differentiate (Kleine-Vehn et al., 2008). Here, in the *pip5k1$^{-/-}$ pip5k2$^{-/-}$* seedlings with a shorter root apical meristem, we observed an abnormally strong
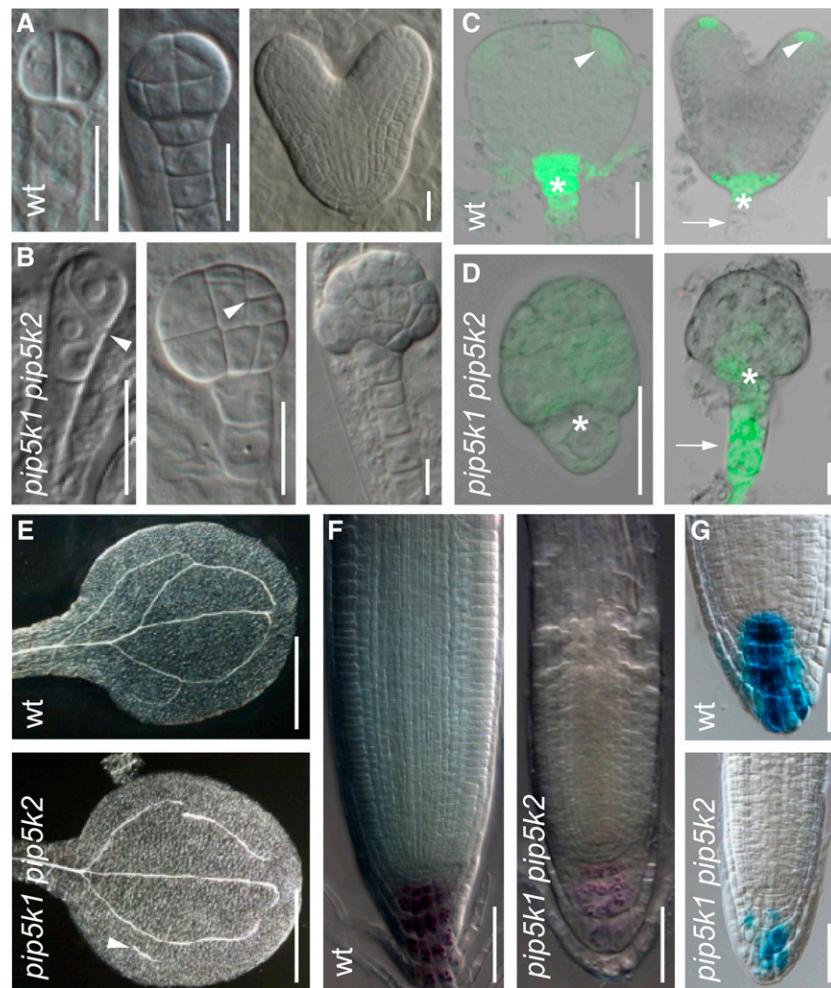
Figure 4. $pip5k1^{-/-}$ $pip5k2^{-/-}$ Mutants Show Multiple Developmental Abnormalities and Ectopic Auxin Response.

Siliques of 6-week-old plants were used to isolate ovules using a binocular stereomicroscope and mounted either directly in a drop of chloral hydrate clearing solution (**[A]** and **[B]**) or an 8% Suc solution (**[C]** and **[D]**). The images were obtained using a DIC-equipped microscope (**[A]** and **[B]**) or a confocal microscope (**[C]** and **[D]**).

(A) and **(B)** Two-celled (left), dermatogen (middle), and torpedo (right) stages of embryo development in wild-type **(A)** and $pip5k1^{-/-}$ $pip5k2^{+/-}$ **(B)** plants. An example of an arrested embryo is shown in the right panel in **(B)**. Arrowheads indicate aberrant cell divisions. Bars = 20 μm.

(C) and **(D)** Auxin-response maxima in embryo visualized by DR5rev:GFP in wild-type **(C)** and $pip5k1^{-/-}$ $pip5k^{-/-}$ **(D)** embryos. Arrowheads highlight the normal DR5 maxima in incipient cotyledons and the future root pole, and arrows indicate the ectopic DR5 response in $pip5k1^{-/-}$ $pip5k2^{-/-}$ embryo suspensor cells. The asterisks mark the position of the hypophysis. Bars = 20 μm.

(E) to **(G)** Seven-day-old seedlings were used to visualize the vascular tissues in cotyledons **(E)** and the root apical meristem size **(F)** and auxin response **(G)**. Seedlings were cleared in 100% ethanol and mounted directly in a drop of chloral hydrate solution **(E)** or mounted directly in the clearing solution after 1 min of Lugol staining **(F)** or overnight GUS staining **(G)**.

(E) and **(F)** $pip5k1^{-/-}$ $pip5k2^{-/-}$ mutants show open vascular loops and vascular islands (**[E]**, arrowhead) in cotyledons. The root apical meristem of the double mutant is smaller than that of the wild type **(F)**. Bars = 50 μm.

(G) Auxin-response maxima visualized by DR5:GUS in wild-type and $pip5k1^{-/-}$ $pip5k2^{-/-}$ root tips. Bars = 50 μm.

lateral signal of PIN2 in cortex cells (Figure 5C), suggesting defects in PIN polarization. This mislocalization was also observed in the otherwise normally patterned root meristems of $pip5k1^{-/-}$ $pip5k2^{-/-}$ seedlings that were phenotypically less affected. During post-embryonic development, the dynamic PIN1 polarization was examined during vascular venation patterning that highly depends on PIN-driven polar auxin transport (Berleth and Mattsson, 2000). In newly forming vascular strands of the wild type, the polar localization

of PIN1 is dynamically established toward the base of previously formed vascular strands (Figure 5D; Scarpella et al., 2006). In contrast with this pattern, in the $pip5k1^{-/-}$ $pip5k2^{-/-}$ mutants, co-ordinated PIN1 polarization did not occur and most of the vascular strands failed to connect (Figure 5D; Supplemental Table 2). This failure is reflected in the formation of vascular islands (Figure 4E) lacking polarized PIN1 distribution (Figure 5D, inset in the left panel). These observations show that bipolar PI4P 5-kinase activity is

required for dynamic PIN polarization during different processes in embryonic and postembryonic development. Apparently, PI4P 5-kinases and PtdIns(4,5)P$_2$ preferentially influence apically–basally localized proteins, because the laterally localized proteins ATP BINDING CASSETTE G37/POLAR AUXIN TRANSPORT INHIBITOR SENSITIVE1, PENETRATION RESISTANCE3 (PEN3), and G-PROTEIN BETA1 (AGB1) and the nonpolar PM H$^+$-ATPase were not affected in the double mutant background (Supplemental Figure 9).

Auxin Modulates Cellular Content and Subcellular Distribution of PIs

The previous results demonstrate the crucial requirement for PIP5K activity in various developmental processes, including those that typically depend on polar localization and dynamic repolarization of PIN proteins, such as embryogenesis (Friml et al., 2003), lateral root and cotyledon organogenesis (Okada et al., 1991; Scarpella et al., 2006), and self-organizing processes of vascular tissue formation (Scarpella et al., 2006). In the canalization hypothesis, auxin is proposed to be the signal that links cell polarity to tissue polarity through a positive effect on its own directional transport (Sachs,

1991). Auxin induces a PIN polarity change in *Arabidopsis* roots manifested by basal-to-lateral repolarization of PIN1 and PIN2 (Sauer et al., 2006a). This effect of auxin is mediated through transcriptional regulation via the TIR1, Aux/IAA, and ARF mechanism and does not involve any known PIN polarity or trafficking regulators. As auxin was shown to regulate the transcript abundance of *PIP5K2* (Mei et al., 2012), we assessed whether auxin might regulate *PIP5K1* transcription and hence influence PIN polarity through the regulation of PI metabolism. We used the promoter fragments fused to the nucleus-localized GUS-GFP reporter gene to visualize the transcriptional response in situ after IAA treatment. We observed that both pPIP5K1:*nls*GUS-GFP and pPIP5K2:*nls*GUS-GFP were induced after 1 h of auxin treatment and remained induced over the 4-h time frame of the experiment (Figures 6A and 6B). Interestingly, pPIP5K2:*nls*GUS-GFP responded by increasing its activity in epidermis and vascular tissues in the root differentiation zone (Figure 6B), suggesting that it may also be involved in differentiation processes in response to auxin. Moreover, our data indicate that *PIP5K1* transcript accumulated within 30 min of auxin treatment and stayed elevated for several hours, after which transcript levels decreased in a pattern similar to
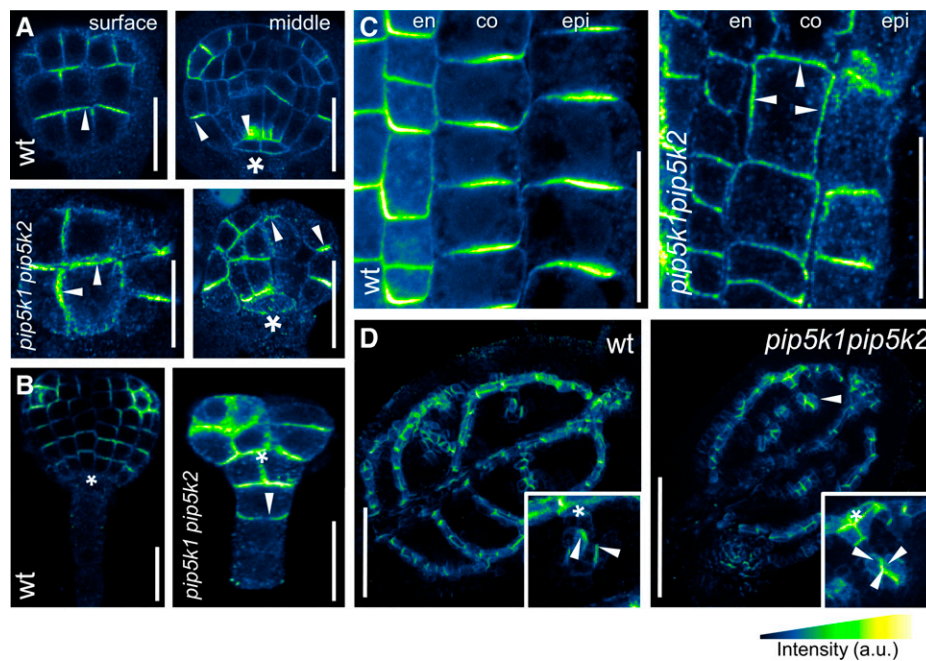

Figure 5. *pip5k1*$^{-/-}$ *pip5k2*$^{-/-}$ Mutants Have PIN Polarity Defects.

(A) and **(B)** Immunolocalization of PIN1 in wild-type and *pip5k1*$^{-/-}$ *pip5k2*$^{-/-}$ mutant embryos. In contrast with the mainly apical polarity of PIN1 in epidermal cells and the basal polarity in procambial cells of wild-type embryos (**[A]**, top panels), the *pip5k1*$^{-/-}$ *pip5k2*$^{-/-}$ embryos displayed more diffuse PIN1 polarizations (**[A]**, bottom panels) and ectopic PIN1 expression in the upper suspensor cells (**[B]**, arrowhead in right panel). Asterisks indicate the hypophysis, and arrowheads highlight PIN polarity. Bars = 20 μm.
(C) PIN immunolocalization in wild-type and *pip5k1*$^{-/-}$ *pip5k2*$^{-/-}$ 7-d-old seedling root tips. In the wild type, PIN1 in endodermis (en) and PIN2 in cortex (co) and epidermis (epi) cells show clear basal and apical localizations, respectively. By contrast, in *pip5k1*$^{-/-}$ *pip5k2*$^{-/-}$ root tips, PIN2 accumulates abnormally at the inner and outer lateral sides of cortex cells (arrowheads). Bars = 50 μm.
(D) Immunolocalization of PIN1 in wild-type (left) and *pip5k1*$^{-/-}$ *pip5k2*$^{-/-}$ (right) primary leaves of 9-d-old seedlings. In the wild type, PIN1 is clearly polarized in the developing vascular tissue pointing toward the leaf base. Newly forming, not yet connected, provascular cells show PIN1 polarization toward older vascular strands (inset). In the *pip5k1*$^{-/-}$ *pip5k2*$^{-/-}$ mutant, PIN1 localization toward the older vascular strands is lost in young, developing vascular tissues (inset). Arrowheads indicate PIN polarity, and asterisks highlight the existing/older vascular strands. Bars = 50 μm.

that of the well-characterized early auxin-inducible genes *SHORT HYPOCOTYL2* (*SHY2*)/*IAA3* and *BODENLOS* (*BDL*)/*IAA12* (Figure 6C). Because auxin-induced PIN repolarization depends on the activity of the transcription factors ARF7 and ARF19 (Sauer et al., 2006a), we analyzed *PIP5K1* auxin inducibility in *arf7 arf19* double mutants. In the *arf7 arf19* double mutants, the induction of *PIP5K1* expression by auxin was largely lost (Figure 6D). Both the naturally occurring auxin IAA (Figures 6C and 6D) and its synthetic analog 1-naphthaleneacetic acid (NAA) (10 μM for 4 h; data not shown) were effective in inducing *PIP5K* transcript accumulation. Overall, the data show that *PIP5K1* is an early auxin-inducible gene, functioning downstream of the auxin signaling pathway known to be required for auxin-dependent PIN polarity rearrangement.

Next, we analyzed whether auxin affected PI levels and/or their subcellular distribution. In wild-type seedlings, exogenous application of 10 μM NAA triggered an ~25% increase in the total level of ^{32}P-labeled PtdIns(4,5)P_2 and a modest (~5%) decrease in the amount of ^{32}P-labeled phosphatidylinositol phosphate (Supplemental Figure 10), substantially reducing the phosphatidylinositol phosphate: PtdIns(4,5)P_2 ratio (~28% reduction) (Figure 7A). This response was lower or lost in the *pip5k1*$^{-/-}$ and *pip5k2*$^{-/-}$ single mutants (Figure 7A; Supplemental Figures 10A and 10B). In the *pip5k2*$^{-/-}$ mutant and partly also in the *pip5k1*$^{-/-}$ *pip5k2*$^{-/-}$ double mutant, the basal levels of ^{32}P-labeled PtdIns(4,5)P_2 increased slightly (Supplemental Figure 10B), which might hint at the upregulated activity of a functionally redundant PI4P 5-kinase isoform. In line with these observations, treatment with IAA (0.1 or 10 μM) for 1 h also caused increases in PtdIns(4,5)P_2 levels (Supplemental Figure 10C), showing that both NAA and IAA have comparable effects on lipid composition. Moreover, we examined the effect of auxin on PIs residing at the PM using the lipid biosensors (Figures 1A and 1C). The PtdIns(4,5)P_2 and PtdIns4P reporters showed distinct changes after 2 h of treatment with 10 μM NAA. Importantly, the YFP-PH$_{PLCδ1}$ signal at the PM was significantly increased with the NAA treatment, whereas YFP-PH$_{FAPP1}$ fluorescence was concomitantly reduced (Figure 7B), suggesting that auxin treatment resulted in a decrease in PtdIns4P (a PIP5K substrate) and an increase in PtdIns(4,5)P_2 (a PIP5K product) at the relevant polar domains of the PM. The combined results show that auxin can regulate the global levels of PtdIns4P and PtdIns(4,5)P_2 at the PM.
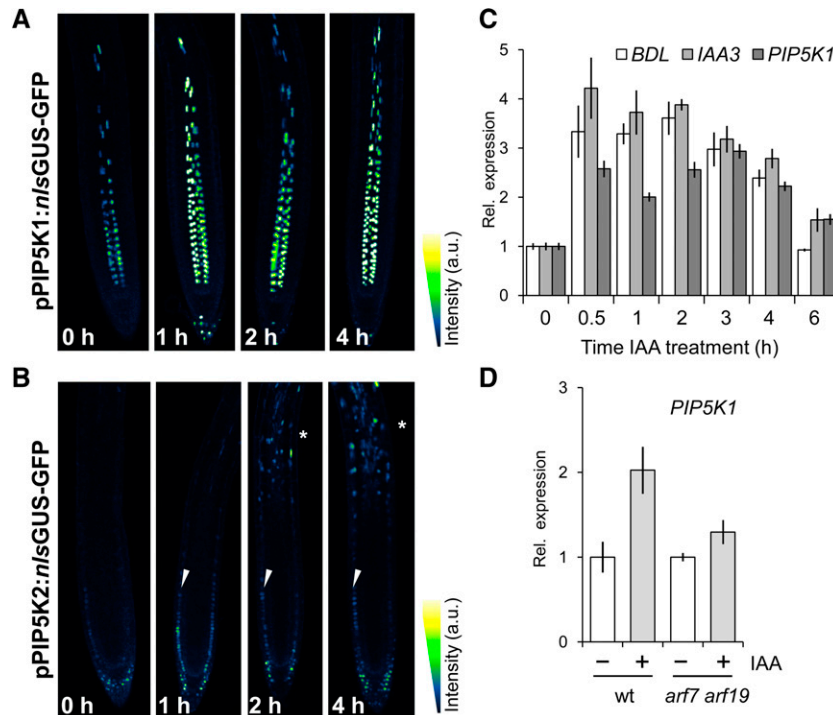

Figure 6. Auxin Modulates *PIP5K* Expression and Transcript Accumulation.

(A) and **(B)** Four-day-old seedlings expressing the transcriptional reporters pPIP5K1:*nls*GUS-GFP **(A)** and pPIP5K2:*nls*GUS-GFP **(B)** were treated in liquid *Arabidopsis* medium containing 10 μM IAA for the times indicated in the bottom left corners and imaged immediately using confocal microscopy. Both transcriptional reporters were induced within 1 h of auxin treatment and maintained their induction over the period of 4 h studied. The pPIP5K2:*nls*GUS-GFP marker was induced in the epidermal cell file (arrowheads in **[B]**) and all over the differentiation zone after 2 h of auxin treatment (asterisks in **[B]**). The fluorescence intensity is indicated as a gradient of color from low (black/dark blue) to high (yellow) fluorescence.
(C) and **(D)** Time-course experiment using 10 μM IAA for the times indicated in **(C)** and for 4 h in **(D)**. RNA extracted from a 1-mm distal section of the root tips of 4-d-old seedlings was used. Means ± SE are presented for three independent experiments. *PIP5K1* transcript accumulated after 0.5 h of IAA treatment, and these levels were maintained over the time course of the experiment; this pattern of transcript accumulation is similar to that observed for the early auxin-inducible genes *BDL* and *IAA3* **(C)**. The *PIP5K1* transcript accumulation after auxin treatment was abolished in *arf7 arf19* double mutants **(D)**.

DISCUSSION

Plants use PI asymmetry at the PM as a way to establish and maintain the polar constitution of tip-growing cells. We show that PtdIns4P and PtdIns(4,5)P_2 together with PIP5K1 and PIP5K2 mark the apical–basal polar domain in the root epidermis, embryos, and lateral root primordia. The PI4P 5-kinase activity is necessary for correct localization of the apical and basal polar cargoes PIN1 and PIN2 and for their dynamic repolarization during different developmental processes, including embryogenesis and vascular tissue formation. We also show that auxin is able to modulate PtdIns4P and PtdIns(4,5)P_2 abundance at the PM, most likely through transcriptional modulation of *PIP5K1* and *PIP5K2* (Mei et al., 2012), providing a transcriptional component of the auxin feedback mechanism on PIN polarity.

PI and PI4P 5-Kinase Localization as a Module for Cell and Tissue Polarity

Advanced imaging revealed that the PI biosensors YFP-PH$_{FAPP1}$ and PH-PH$_{PLC\delta1}$ are localized at the PM in root cells in a bipolar fashion, enriched at both the apical and basal cell sides of root cells (Figure 1; Supplemental Figures 1 and 2). To best support this claim, we analyzed the biosensor lines published before (van Leeuwen et al., 2007; Vermeer at al., 2009; Simon et al., 2014) as well as a new set of markers that we generated using a different constitutive promoter (pUBQ10). Overall, our analysis included multiple lines with different expression levels, and in both set of markers we consistently observed the bipolar enrichment of PtdIns4P and PtdIns(4,5)P_2 sensors in epidermal cells of the root apical meristem (Figures 1 and 3). Moreover, we have confirmed the bipolar localization by immunolocalization using antibodies against PtdIns4P and PtdIns(4,5)P_2 (Supplemental Figure 3). In addition, the PI4P 5-kinases PIP5K1 and PIP5K2 were also bipolarly localized at the PM in root apical meristem cells and displayed pronounced bipolar localization throughout lateral root primordium development and in embryos (Figure 2). The bipolar PI localization is consistent with the localization of PIP5K1 and PIP5K2 in root cells, so even though we were not able to clearly observe the PI distribution in every cell type of the plant due to technical limitations, it appears reasonable to assume that PtdIns(4,5)P_2 distribution will follow the localization of the PI4P 5-kinases, as these enzymes are the only known source of PtdIns(4,5)P_2 in plants (Mueller-Roeber and Pical, 2002). In line with this observation, recent evidence from studies on tip-growing plant cells suggests that PtdIns(4,5)P_2 does not freely diffuse from its site of production but instead is channeled toward specific downstream effectors by processes depending on the interaction of PI4P 5-kinases with these targets (Stenzel et al., 2012; Heilmann and Heilmann, 2013). The channeling hypothesis is consistent with the notion that PtdIns(4,5)P_2 will colocalize with PI4P 5-kinases, as has been observed previously in tobacco (*Nicotiana tabacum*) pollen tubes (Ischebeck et al., 2008, 2011) and *Arabidopsis* root hairs (van Leeuwen et al., 2007; Thole et al., 2008; Vermeer et al., 2009). Therefore, the bipolar PI and PI4P 5-kinase localization in the root apical meristem suggests that PI compartmentalization occurs in cells within a multicellular tissue context in a similar way to that in tip-growing cells (Kost et al., 1999; Ischebeck et al., 2008, 2011; Sousa et al., 2008; Munnik and Nielsen, 2011). This implies the existence of

a so-far unappreciated lipid signaling module important for cell polarity in the establishment of various multicellular plant tissues.

PIs and Auxin Signaling in Plant Development

Previous reports had highlighted the importance of PIs in auxin-mediated development (Xue et al., 2007). Several of the phenotypes described here for the *pip5k1$^{-/-}$ pip5k2$^{-/-}$* double mutants resemble those found for mutants deficient in auxin biosynthesis, auxin transport, and auxin signaling (Friml et al., 2003; Blilou et al., 2005; Scarpella et al., 2006; Weijers et al., 2006; Stepanova et al., 2008; Won et al., 2011; Robert et al., 2013), suggesting that there is a link between PI4P 5-kinase activity and auxin. The relevant phenotypes include early and late defects in embryogenesis, disconnected vascular tissues, reduced root apical meristem size, root length and lateral root density, and defects in seedling development (Figure 4; Supplemental Figure 8). In addition, we observed reduced or defective local auxin responses in embryos and roots. Generally, the embryos were more affected in both auxin response and patterning compared with the roots, indicating
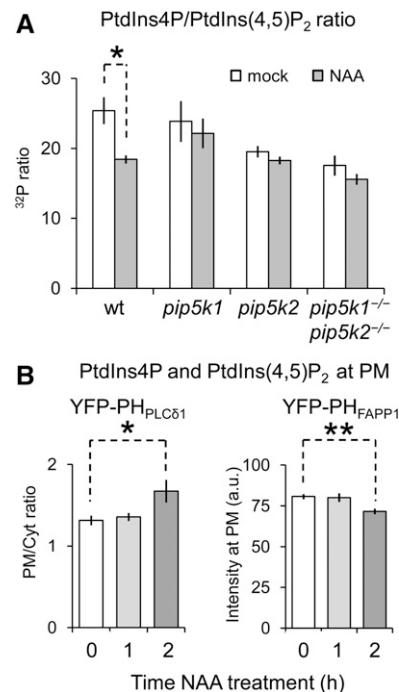

Figure 7. Auxin Modulates PI Levels at the PM.

(A) Total PI amounts measured in 5-d-old seedlings of the wild type and *pip5k* mutants before and after treatment with 10 μM NAA for 30 min. Auxin reduced the PtdIns(4,5)P_2 levels, indicated here by a 28% reduction in the PtdIns4P:PtdIns(4,5)P_2 ratio in the wild type (see Supplemental Figure 10 for specific data). The single and double *pip5k* mutants failed to respond to auxin by increasing the amounts of PIs. A two-tailed Student's *t* test was used; *P < 0.05.

(B) Quantification of the effect of auxin on PtdIns(4,5)P_2 and PtdIns4P at the PM as visualized by the PI markers p35S:YFP-PH$_{PLC\delta1}$ and p35S: YFP-PH$_{FAPP1}$, respectively. A two-tailed Student's *t* test was used; *P < 0.05, **P < 0.01. See Methods for details.

a higher degree of functional redundancy in the PI4P 5-kinase family during postembryonic development.

The $pip5k1^{-/-}$ $pip5k2^{-/-}$ mutant phenotypes and aberrant spatial patterns of auxin responses indicate a defect in auxin transport and/or signaling as a major underlying cause of the developmental defects. However, other cellular processes may also contribute to those phenotypes, since PIs can interfere with the activity of various other PM proteins. For instance, the type 2C protein phosphatases POLTERGEIST (POL) and POL-like (PLL) are PM localized, and their activity is modulated by the direct binding of phosphatidylinositol monophosphates, such as PtdIns4P (Gagne and Clark, 2010). POL/PLL redundantly influence meristem activity by regulating *WUS/WOX5* expression and stem cell maintenance (Song et al., 2008). Importantly, *pol pll* double mutants have defects in key asymmetric early divisions during embryogenesis, interfering with auxin gradients and PIN1 expression necessary to establish the root pole and vascular tissues. Although POL/PLL do not seem to interact physically with PtdIns(4,5)P$_2$ (Gagne and Clark, 2010), the activity of PI4P 5-kinases may regulate POL/PLL action by directly modulating the PtdIns4P pool.

PI4P 5-Kinase Activity Is Required for PIN Polarity

Auxin transport and its directionality are dependent on the polar localization of PIN auxin transporters (Petrásek et al., 2006; Wisniewska et al., 2006). We observed that PIN polarity is altered in the $pip5k1^{-/-}$ $pip5k2^{-/-}$ double mutant (Figure 5), providing a rationale for the morphological phenotypes and defective auxin-response distribution. Nonetheless, it remains unclear by which mechanism PtdIns(4,5)P$_2$ acts on PIN and cell polarity. PtdIns(4,5)P$_2$ may directly bind an effector that influences PIN polarity or trafficking, or alternatively, PtdIns(4,5)P$_2$ may be involved in the local production of second messengers important for PIN polarity or trafficking.

In previous work on tip-growing plant cells, PI4P 5-kinases and PtdIns(4,5)P$_2$ were implicated in the control of exocytosis (Ischebeck et al., 2008, 2010) as well as clathrin-mediated endocytosis and membrane recycling (König et al., 2008; Sousa et al., 2008; Zhao et al., 2010; Mei et al., 2012). During cytokinesis of tobacco BY-2 cells, PtdIns(4,5)P$_2$ has been shown to lead the expanding cell plate, while PtdIns4P was localized there from the start (van Leeuwen et al., 2007; Vermeer et al., 2009). Recent reports indicate that PtdIns(4,5)P$_2$ and PI4P 5-kinases may be involved in the regulation of PIN1, PIN2, and PIN3 trafficking during the gravitropic bending response (Mei et al., 2012; Ischebeck and Werner et al., 2013), highlighting the hypothesis of an indirect effect of PIs and PI4P 5-kinases on PIN polarity through the modulation of endosomal trafficking. The observations that auxin can induce the transcription of *PIP5K1* and *PIP5K2* (Figure 6; Mei et al., 2012) and modulate the global content and PM levels of PtdIns(4,5)P$_2$ (Figure 7) suggest an auxin input into the PtdIns(4,5)P$_2$ cell polarity module, thus contributing to the feedback regulation of auxin transport directionality.

The polarization of PIN proteins depends on endosomal recycling events that are mediated by clathrin-mediated endocytosis. It was recently reported that the PM focal distribution patterns of the clathrin light chain are perturbed in the $pip5k1^{-/-}$ $pip5k2^{-/-}$ double mutant and that this has detrimental effects on the formation of brefeldin A–dependent endosomal bodies labeled by fluorescence-

tagged PIN1 and PIN2 (Ischebeck and Werner et al., 2013). These results are highly complementary to our findings and indicate that the defects in auxin-dependent development reported here for the $pip5k1^{-/-}$ $pip5k2^{-/-}$ double mutant might be related to defects in clathrin-mediated endocytosis and the recycling of PIN proteins. Another possible link between PIs and the control of cell polarity is via the protein kinase PINOID (PID). PID is one of the few molecular players directly involved in PIN polarity determination. PID directly phosphorylates the central hydrophilic loop of the PINs, thereby enhancing PIN trafficking toward the apical cell side (Friml et al., 2004; Michniewicz et al., 2007). The *Arabidopsis* homolog of the mammalian 3-PHOSPHOINOSITIDE-DEPENDENT PROTEIN KINASE1 (PDK1) is required for the activation of PID (Zegzouti et al., 2006). Importantly, PDK1 is able to bind PtdOH and several PIs, including PtdIns4P and PtdIns(4,5)P$_2$ (Deak et al., 1999; Bögre et al., 2003). Therefore, PIs may work as scaffolding signals to recruit PDK1 and enhance PID activity, thus affecting apical–basal PIN polarization. Alternatively, the hydrolysis of PtdIns4P or PtdIns(4,5)P$_2$ by PI-specific phospholipase C (PLC) may lead to the biosynthesis of diacylglycerol and inositol 4,5-bisphosphate or inositol 1,4,5-trisphosphate, which can be phosphorylated further into PtdOH and soluble inositol polyphosphates, which have all been implicated in signaling (reviewed in Munnik and Vermeer, 2010; Munnik, 2014). For example, inositol hexakisphosphate can release intracellular Ca^{2+} (Lemtiri-Chlieh et al., 2003) and seems to be structurally required for TIR1 function (Tan et al., 2007). Genetic evidence suggests crosstalk of inositol polyphosphate and auxin signaling. For instance, several inositol phosphate 5-phosphatase mutants display altered auxin levels and responses (Carland and Nelson., 2004; Lin et al., 2005; Chen et al., 2008; Wang et al., 2009; Robles et al., 2010; Zhang et al., 2011). Regardless of the exact mode of action, all these observations point to a regulatory loop involving PM-associated PIs that modulate apical–basal PIN polarity via crosstalk between lipid signaling and the PIN polarizing machinery.

METHODS

Plant Material and Growth Conditions

All *Arabidopsis thaliana* lines were in the Columbia background, and $pip5k1^{-/-}$ and $pip5k2^{-/-}$ were the insertional mutants SALK_146728 and SALK_012487, respectively, obtained from the ABRC. The T-DNA *pip5k* mutants were genotyped using the LBa1 primer and the gene-specific primers listed in Supplemental Table 3. The *arf7 arf19* double mutant has been described (Okushima et al., 2005). The marker lines DR5:GUS (Ulmasov et al., 1997), DR5rev:GFP (Friml et al., 2003), aqPIP2-GFP (Cutler et al., 2000), p35S:YFP-PH$_{PLCδ1}$ (van Leeuwen et al., 2007), p35S: YFP-PH$_{FAPP1}$ (Vermeer et al., 2009), and pUBQ10:CITRINE-PH$_{PLCδ1}$ (Simon et al., 2014) were obtained from the respective authors and introgressed (when appropriate) into the double $pip5k1^{+/-}$ $pip5k2^{-/-}$ mutant by crossing.

Seeds were sterilized overnight by chlorine gas, sown on solid *Arabidopsis* medium (one-half-strength Murashige and Skoog basal salts, 1% Suc, and 0.8% agar, pH 5.7), and stratified at 4°C for at least 2 d prior to transfer to a growth room with a 16-h-light/8-h-dark illumination regime at 18°C. The seedlings were grown vertically for 4 d unless the assay required the use of $pip5k1^{-/-}$ $pip5k2^{-/-}$, in which case the seedlings were grown for 7 to 9 d to allow clear discrimination of the double mutant phenotype.

Generation of Constructs for PI and PIP5K Fluorescent Markers

To clone all promoters (*DNAJc17* [AT5G23590], *PIP5K1*, and *PIP5K2* promoters), we designed primers to cover from −1 to −2000 bp upstream of the gene's ATG codon and PCR amplified and recombined the products using the Gateway BP Clonase II Enzyme Mix (Invitrogen) into the entry vector pDONRP4P1r. To generate the GUS-GFP reporter constructs, the promoter-pDONRP4P1r entry clones were recombined with pEN-L1-NSF-L2 using the Gateway LR Clonase II Enzyme Mix (Invitrogen).

To generate the YFP-PIP5K constructs, first we subcloned the YFP-PIP5K fusions by PCR amplification of YFP-PIP5K from pMDC7(YFP-PIP5K) plasmids (Ischebeck and Werner et al., 2013) and recombined them into the entry vector pDONR221 using the Gateway BP Clonase II Enzyme Mix (Invitrogen). Then we recombined these plasmids with the respective promoter cloned in the entry vector pDORNP4P1r (described above) and the destination vector pB7m24GW using the Gateway LR Clonase II Enzyme Mix (Invitrogen).

To generate pUBQ10:YFP-PH$_{PLC\delta1}$ and pUBQ10:YFP-PH$_{FAPP1}$, the corresponding lipid binding domains PH$_{PLC\delta1}$ and PH$_{FAPP1}$ were PCR amplified, cloned into pUNI51, and recombined into pNIGEL07 using the CRE/lox system as described previously (Geldner et al., 2009).

Standard cloning methods were used, mostly the Gateway cloning system (Invitrogen) and the iPROOF DNA polymerase (Bio-Rad) for PCR amplifications, following the manufacturers' instructions. All plasmids were sequenced to confirm the absence of point mutations in the PCR-amplified sequences prior to transformation into *Arabidopsis* Columbia using the floral dip method (Clough and Bent, 1998). All primers used are listed in Supplemental Table 3.

Immunolocalization, GUS Staining, and Live Cell Imaging

PIN immunolocalizations of primary root, embryo, and leaf vasculature were performed as described (Sauer et al., 2006b). The antibodies were used in the following dilutions: anti-PIN1, 1:1000 (Paciorek et al., 2005); anti-PIN2, 1:1000 (Abas et al., 2006); anti-PIS, 1:600 (Ito and Gray, 2006); anti-PEN3, 1:400 (Agrisera); anti-AGB1, 1:400 (Agrisera); and anti–PM H$^+$-ATPase, 1:600 (Agrisera). In all cases, the secondary anti-rabbit antibody coupled to Cy3 (Sigma-Aldrich) or Alexa488 (Molecular Probes) was diluted 1:600. Lipid immunostaining was performed using a protocol adapted from Hammond et al. (2009). Briefly, 4-d-old seedlings were fixed in 4% paraformaldehyde and 0.25% glutaraldehyde in buffer A (20 mM PIPES, pH 6.8, 137 mM NaCl, and 2.7 mM KCl) under vacuum for 45 min, then cells were permeabilized by incubation with 2% Driselase at room temperature for 30 min and a solution of buffer A containing 50 mM NH$_4$Cl and 0.5% saponin for 45 min. After a preincubation with buffer A containing 3% BSA plus 0.1% saponin, the samples were incubated for 24 h in the primary antibodies diluted in buffer A containing 5% BSA [anti-PtdIns(4,5)P$_2$ IgM, 1:20; and anti-PtdIns4P IgM, 1:20 [Echelon]] at 4°C, and after washing the samples in buffer A, they were incubated for 6 h in Cy3-coupled secondary antibodies (Sigma-Aldrich) diluted 1:600 in buffer A and 5% BSA.

Staining with GUS was done as described (Swarup et al., 2008). The root tips were mounted in chloral hydrate and visualized using a microscope (Olympus BX51) equipped with differential interference contrast (DIC). Whole seedlings and embryos were cleared poststaining using absolute ethanol, and then the samples were rehydratated in a gradient of ethanol in water (75, 50, 25, and 0%), incubating 30 to 60 min each time. The samples were mounted in chloral hydrate solution and visualized using a DIC microscope (Olympus BX51).

For live imaging of the phosphatidylinositol markers, seedlings at 4 d after germination were mounted in a drop of *Arabidopsis* medium and visualized immediately using a Zeiss 710 confocal microscope. Root cells were imaged within the root apical meristem zone (i.e., the cell-proliferating region) using a 63-μm pinhole, C-Apochromat 63×/1.20 water-immersion objective (Zeiss). YFP was excited using a 514-nm

argon ion laser line, fluorescence was detected using a 540/20-nm bandpass filter, and each scan was the result of averaging 16 frames to produce low-noise images. The surface of the cells was carefully acquired when observing the root epidermal cells, whereas a middle section of the cells was used when imaging all other cell types.

The 3D reconstructions of XVE>PIP5K1-YFP, pUBQ10:YFP-PH$_{FAPP1}$, and pUBQ10: CITRINE-PH$_{PLC\delta1}$ were performed with a spinning disc microscope (Andor Spinning Disc System) with an inverted Zeiss observer using a C-Apochromat 63×/1.2 water objective. Three-day-old XVE>-PIP5K1-YFP seedlings were treated with 2.5 μM estradiol in liquid plant growth medium overnight before observation.

Auxin Treatments and PI Analysis

Radioactive PtdInsP$_2$ levels were measured by labeling 5-d-old seedlings (three per tube in triplicate) with 10 μCi of carrier-free ^{32}P-labeled ortho-phosphate overnight (~16 h) as described previously (Munnik and Zarza, 2013). The next day, seedlings were treated with 10 μM NAA for 30 min, after which lipids were extracted, separated by thin layer chromatography, and quantified by orthophosphate imaging (Munnik and Zarza, 2013).

Alternatively, nonradioactive PtdInsP$_2$ levels were measured by means of their fatty acid content. In that case, 50 to 60 seedlings per sample were transferred to solid medium supplemented with 0.1 or 10 μM IAA. After 1 h, seedlings were harvested and the total fresh weight was determined. PtdInsP$_2$ was extracted and analyzed as described (König et al., 2008).

The PI changes at the PM upon auxin treatments were determined as follows using the biosensors expressed under the control of the 35S promoter. Four days after germination, seedlings were incubated for the indicated times in liquid *Arabidopsis* medium containing 10 μM NAA and immediately imaged using a Zeiss 710 confocal microscope equipped with a 63× water-immersion lens (Zeiss) using identical imaging conditions for all samples. The images were analyzed with the ImageJ software (http://rsb.info.nih.gov/ij/). The PtdIns4P marker showed fairly constant fluorescence intensity in all cells in root epidermis, so the fluorescence was directly compared at the PM between NAA treatments and controls. By contrast, the PtdIns(4,5)P$_2$ marker showed more variable fluorescence intensity, an intense cytosolic fraction besides the one attached to the PM, so a different approach was used. The cells that strongly expressed the PtdIns(4,5)P$_2$ marker were selected to allow more reliable quantification, and the PM fluorescence intensity was measured and calculated as the ratio between this PM intensity and the average fluorescence intensity of the adjacent cytoplasm measured by the circumference of a constant arbitrary size of 5 μm in diameter. This ratio allowed normalization of the fluorescence signal to the relative expression level per cell. For both PI markers, the fluorescence intensity was measured at the PM using a three-pixel-wide line covering the whole axial membrane of all root epidermal cells in focus included in a single confocal image. All measured cells were used to calculate the average signal per root and then to obtain the mean of 10 roots per time point. These experiments were done in three biological replicates.

Transcript Level Analysis

Total RNA was extracted with the RNeasy Mini kit (Qiagen). For quantitative RT-PCR, poly(dT) cDNA was prepared from 1 μg of total RNA with the iScript cDNA synthesis kit (Bio-Rad) and quantified on the LightCycler 480 (Roche) with the qPCR LightCycler 480 SYBR Green I Master (Roche). PCR was run on 384-well reaction plates that were heated for 10 min to 95°C, followed by 45 denaturation cycles of 10 s at 95°C, annealing for 15 s at 60°C, and extension for 15 s at 72°C. Targets were quantified with specific primer pairs designed with Beacon Designer 4.0 (Premier Biosoft International). Expression levels were normalized to *CAP BINDING PROTEIN20* (*CBP20*; AT5G44200) and *ELONGATION FACTOR4-α* (*eIF4A*; AT1G54270), which were constitutively expressed across samples. All PCRs were run in three technical repeats, and the data were processed with

qBase version 1.3.4 (Hellemans et al., 2007). The primers used are listed in Supplemental Table 3.

Accession Numbers

Sequence data from this article can be found in the Arabidopsis Genome Initiative or GenBank/EMBL databases under the following accession numbers: *ACTIN8*, AT1G49240; *BDL/IAA12*, AT1G04550; *CBP20*, AT5G44200; *DNAJc17*, AT5G23590; *EIF4A*, AT1G54270; *SHY2/IAA3*, AT1G04240; *PIP5K1*, At1g21980; *PIP5K2*, At1g77740; *PIN1*, At1g73590; and *PIN2*, At5g57090.

Supplemental Data

The following materials are available in the online version of this article.

Supplemental Figure 1. 3D Reconstructions of Root Epidermal Cells Imaged by Confocal Microscopy of Seedlings Expressing the Phosphoinositide Biosensors.

Supplemental Figure 2. 3D Reconstructions of PIP5K Marker Lines and Phosphoinositide Biosensors Imaged by Spinning Disc Microscopy.

Supplemental Figure 3. Whole-Mount Immunolocalization on Epidermal Cells on 4-d-Old Seedling Root Tips Using Anti-PtdIns(4,5)P_2 and Anti-PtdIns4P Antibodies.

Supplemental Figure 4. Expression Patterns of pPIP5K1:GUS and pPIP5K2:GUS in Root Tips, Cotyledon Vasculature, and during Early Embryo Development.

Supplemental Figure 5. Functional Complementation of *pip5k1$^{-/-}$ pip5k2$^{-/-}$* Double Mutants with the pPIP5K1:YFP-PIP5K1 Construct.

Supplemental Figure 6. Root Whole-Mount Immunolocalization on 4-d-Old Seedlings of pPIP5K1:YFP-PIP5K1 and pPIP5K2:YFP-PIP5K2 Using Anti-PIN1, Anti-PIN2, and Anti-GFP Antibodies.

Supplemental Figure 7. Apical-to-Lateral Fluorescence Ratio (Polarity Index) of Phosphoinositide Biosensors Expressed under the Control of the 35S Promoter and PIP5K1 Proteins in Root Epidermis and Procambial Cells Expressed under the Control of the *DNAJc17* Promoter.

Supplemental Figure 8. Characterization of *pip5k* Mutants.

Supplemental Figure 9. Apolar and Outer Lateral Localized Proteins Are Not Affected in the *pip5k1$^{-/-}$ pip5k2$^{-/-}$* Double Mutant.

Supplemental Figure 10. Phosphoinositide Measurements in Response to Auxin in Wild-Type and *pip5k* Mutant Seedlings.

Supplemental Table 1. Mutant Phenotype Segregation in Seedlings and Embryos in the Wild Type and the *pip5k1$^{-/-}$ pip5k2$^{+/-}$* Double Mutant.

Supplemental Table 2. The *pip5k1$^{-/-}$ pip5k2$^{-/-}$* Mutant Frequently Has Disconnected Provascular Fragments as Well as Reduced Complexity in the Vascular Tissues (i.e., Reduced Branching Points, Secondary Veins, and Closed Areoles).

Supplemental Table 3. Primer Sequences Used for Expression Analysis and Cloning Procedures.

AUTHOR CONTRIBUTIONS

R.T., M.S., I.H., and J.F. conceived the project. R.T., S.V., M.P.-G., H.L., M.H., R.v.W., and J.E.M.V. carried out the experiments. R.T., M.H., R.v. W., I.H., and T.M. analyzed the data. R.T. and J.F. wrote the article.

REFERENCES

Abas, L., Benjamins, R., Malenica, N., Paciorek, T., Wiśniewska, J., Moulinier-Anzola, J.C., Sieberer, T., Friml, J., and Luschnig, C. (2006). Intracellular trafficking and proteolysis of the *Arabidopsis* auxin-efflux facilitator PIN2 are involved in root gravitropism. Nat. Cell Biol. **8:** 249–256.

Assémat, E., Bazellières, E., Pallesi-Pocachard, E., Le Bivic, A., and Massey-Harroche, D. (2008). Polarity complex proteins. Biochim. Biophys. Acta **1778:** 614–630.

Balla, J., Kalousek, P., Reinöhl, V., Friml, J., and Procházka, S. (2011). Competitive canalization of PIN-dependent auxin flow from axillary buds controls pea bud outgrowth. Plant J. **65:** 571–577.

Baster, P., Robert, S., Kleine-Vehn, J., Vanneste, S., Kania, U., Grunewald, W., De Rybel, B., Beeckman, T., and Friml, J. (2013). SCF(TIR1/AFB)-auxin signalling regulates PIN vacuolar trafficking and auxin fluxes during root gravitropism. EMBO J. **32:** 260–274.

Benková, E., Michniewicz, M., Sauer, M., Teichmann, T., Seifertová, D., Jürgens, G., and Friml, J. (2003). Local, efflux-dependent auxin gradients as a common module for plant organ formation. Cell **115:** 591–602.

Berleth, T., and Mattsson, J. (2000). Vascular development: Tracing signals along veins. Curr. Opin. Plant Biol. **3:** 406–411.

Blilou, I., Xu, J., Wildwater, M., Willemsen, V., Paponov, I., Friml, J., Heidstra, R., Aida, M., Palme, K., and Scheres, B. (2005). The PIN auxin efflux facilitator network controls growth and patterning in *Arabidopsis* roots. Nature **433:** 39–44.

Bögre, L., Okrész, L., Henriques, R., and Anthony, R.G. (2003). Growth signalling pathways in *Arabidopsis* and the AGC protein kinases. Trends Plant Sci. **8:** 424–431.

Braun, M., Baluska, F., von Witsch, M., and Menzel, D. (1999). Redistribution of actin, profilin and phosphatidylinositol-4,5-bisphosphate in growing and maturing root hairs. Planta **209:** 435–443.

Carland, F.M., and Nelson, T. (2004). Cotyledon vascular pattern2-mediated inositol (1,4,5) triphosphate signal transduction is essential for closed venation patterns of *Arabidopsis* foliar organs. Plant Cell **16:** 1263–1275.

Chapman, E.J., and Estelle, M. (2009). Mechanism of auxin-regulated gene expression in plants. Annu. Rev. Genet. **43:** 265–285.

Chen, X., Lin, W.H., Wang, Y., Luan, S., and Xue, H.W. (2008). An inositol polyphosphate 5-phosphatase functions in PHOTOTROPIN1 signaling in *Arabidopsis* by altering cytosolic Ca^{2+}. Plant Cell **20:** 353–366.

Clough, S.J., and Bent, A.F. (1998). Floral dip: A simplified method for *Agrobacterium*-mediated transformation of *Arabidopsis thaliana*. Plant J. **16:** 735–743.

Cutler, S.R., Ehrhardt, D.W., Griffitts, J.S., and Somerville, C.R. (2000). Random GFP::cDNA fusions enable visualization of subcellular structures in cells of *Arabidopsis* at a high frequency. Proc. Natl. Acad. Sci. USA **97:** 3718–3723.

Deak, M., Casamayor, A., Currie, R.A., Downes, C.P., and Alessi, D.R. (1999). Characterisation of a plant 3-phosphoinositide-dependent protein kinase-1 homologue which contains a pleckstrin homology domain. FEBS Lett. **451:** 220–226.

Dettmer, J., and Friml, J. (2011). Cell polarity in plants: When two do the same, it is not the same.... Curr. Opin. Cell Biol. **23:** 686–696.

Dieck, C.B., Boss, W.F., and Perera, I.Y. (2012). A role for phosphoinositides in regulating plant nuclear functions. Front. Plant Sci. **3:** 50.

Di Paolo, G., and De Camilli, P. (2006). Phosphoinositides in cell regulation and membrane dynamics. Nature **443:** 651–657.

Dowd, P.E., Coursol, S., Skirpan, A.L., Kao, T.H., and Gilroy, S. (2006). Petunia phospholipase c1 is involved in pollen tube growth. Plant Cell **18:** 1438–1453.

Elge, S., Brearley, C., Xia, H.J., Kehr, J., Xue, H.W., and Mueller-Roeber, B. (2001). An *Arabidopsis* inositol phospholipid kinase strongly expressed in procambial cells: Synthesis of PtdIns(4,5)P$_2$ and PtdIns(3,4,5)P$_3$ in insect cells by 5-phosphorylation of precursors. Plant J. **26:** 561–571.

Friml, J., Vieten, A., Sauer, M., Weijers, D., Schwarz, H., Hamann, T., Offringa, R., and Jürgens, G. (2003). Efflux-dependent auxin gradients establish the apical-basal axis of *Arabidopsis*. Nature **426:** 147–153.

Friml, J., et al. (2004). A PINOID-dependent binary switch in apical-basal PIN polar targeting directs auxin efflux. Science **306:** 862–865.

Gagne, J.M., and Clark, S.E. (2010). The *Arabidopsis* stem cell factor POLTERGEIST is membrane localized and phospholipid stimulated. Plant Cell **22:** 729–743.

Gassama-Diagne, A., Yu, W., ter Beest, M., Martin-Belmonte, F., Kierbel, A., Engel, J., and Mostov, K. (2006). Phosphatidylinositol-3,4,5-trisphosphate regulates the formation of the basolateral plasma membrane in epithelial cells. Nat. Cell Biol. **8:** 963–970.

Geldner, N. (2009). Cell polarity in plants: A PARspective on PINs. Curr. Opin. Plant Biol. **12:** 42–48.

Geldner, N., Dénervaud-Tendon, V., Hyman, D.L., Mayer, U., Stierhof, Y.D., and Chory, J. (2009). Rapid, combinatorial analysis of membrane compartments in intact plants with a multicolor marker set. Plant J. **59:** 169–178.

Hammond, G.R., Schiavo, G., and Irvine, R.F. (2009). Immunocytochemical techniques reveal multiple, distinct cellular pools of PtdIns4P and PtdIns(4,5)P$_2$. Biochem. J. **422:** 23–35.

Heilmann, I. (2009). Using genetic tools to understand plant phosphoinositide signalling. Trends Plant Sci. **14:** 171–179.

Heilmann, M., and Heilmann, I. (2013). Arranged marriage in lipid signalling? The limited choices of PtdIns(4,5)P$_2$ in finding the right partner. Plant Biol. (Stuttg.) **15:** 789–797.

Heisler, M.G., Ohno, C., Das, P., Sieber, P., Reddy, G.V., Long, J.A., and Meyerowitz, E.M. (2005). Patterns of auxin transport and gene expression during primordium development revealed by live imaging of the Arabidopsis inflorescence meristem. Curr. Biol. **15:** 1899–1911.

Hellemans, J., Mortier, G., De Paepe, A., Speleman, F., and Vandesompele, J. (2007). qBase relative quantification framework and software for management and automated analysis of real-time quantitative PCR data. Genome Biol. **8:** R19.1–R19.14.

Helling, D., Possart, A., Cottier, S., Klahre, U., and Kost, B. (2006). Pollen tube tip growth depends on plasma membrane polarization mediated by tobacco PLC3 activity and endocytic membrane recycling. Plant Cell **18:** 3519–3534.

Ikeda, Y., Men, S., Fischer, U., Stepanova, A.N., Alonso, J.M., Ljung, K., and Grebe, M. (2009). Local auxin biosynthesis modulates gradient-directed planar polarity in *Arabidopsis*. Nat. Cell Biol. **11:** 731–738.

Ischebeck, T., Seiler, S., and Heilmann, I. (2010). At the poles across kingdoms: Phosphoinositides and polar tip growth. Protoplasma **240:** 13–31.

Ischebeck, T., Stenzel, I., and Heilmann, I. (2008). Type B phosphatidylinositol-4-phosphate 5-kinases mediate *Arabidopsis* and *Nicotiana tabacum* pollen tube growth by regulating apical pectin secretion. Plant Cell **20:** 3312–3330.

Ischebeck, T., Stenzel, I., Hempel, F., Jin, X., Mosblech, A., and Heilmann, I. (2011). Phosphatidylinositol-4,5-bisphosphate influences Nt-Rac5-mediated cell expansion in pollen tubes of *Nicotiana tabacum*. Plant J. **65:** 453–468.

Ischebeck, T., et al. (2013). Phosphatidylinositol 4,5-bisphosphate influences PIN polarization by controlling clathrin-mediated membrane trafficking in *Arabidopsis*. Plant Cell **25:** 4894–4911.

Ito, H., and Gray, W.M. (2006). A gain-of-function mutation in the *Arabidopsis* pleiotropic drug resistance transporter PDR9 confers resistance to auxinic herbicides. Plant Physiol. **142:** 63–74.

Kitakura, S., Vanneste, S., Robert, S., Löfke, C., Teichmann, T., Tanaka, H., and Friml, J. (2011). Clathrin mediates endocytosis and polar distribution of PIN auxin transporters in *Arabidopsis*. Plant Cell **23:** 1920–1931.

Kleine-Vehn, J., Langowski, L., Wisniewska, J., Dhonukshe, P., Brewer, P.B., and Friml, J. (2008). Cellular and molecular requirements for polar PIN targeting and transcytosis in plants. Mol. Plant **1:** 1056–1066.

Kleine-Vehn, J., et al. (2011). Recycling, clustering, and endocytosis jointly maintain PIN auxin carrier polarity at the plasma membrane. Mol. Syst. Biol. **7:** 540.

König, S., Hoffmann, M., Mosblech, A., and Heilmann, I. (2008). Determination of content and fatty acid composition of unlabeled phosphoinositide species by thin-layer chromatography and gas chromatography. Anal. Biochem. **378:** 197–201.

Kost, B., Lemichez, E., Spielhofer, P., Hong, Y., Tolias, K., Carpenter, C., and Chua, N.H. (1999). Rac homologues and compartmentalized phosphatidylinositol 4,5-bisphosphate act in a common pathway to regulate polar pollen tube growth. J. Cell Biol. **145:** 317–330.

Kusano, H., Testerink, C., Vermeer, J.E., Tsuge, T., Shimada, H., Oka, A., Munnik, T., and Aoyama, T. (2008). The *Arabidopsis* phosphatidylinositol phosphate 5-kinase PIP5K3 is a key regulator of root hair tip growth. Plant Cell **20:** 367–380.

Lemtiri-Chlieh, F., MacRobbie, E.A., Webb, A.A., Manison, N.F., Brownlee, C., Skepper, J.N., Chen, J., Prestwich, G.D., and Brearley, C.A. (2003). Inositol hexakisphosphate mobilizes an endomembrane store of calcium in guard cells. Proc. Natl. Acad. Sci. USA **100:** 10091–10095.

Li, G., and Xue, H.W. (2007). *Arabidopsis PLDζ2* regulates vesicle trafficking and is required for auxin response. Plant Cell **19:** 281–295.

Li, R., and Bowerman, B. (2010). Symmetry breaking in biology. Cold Spring Harb. Perspect. Biol. **2:** a003475.

Lin, W.H., Wang, Y., Mueller-Roeber, B., Brearley, C.A., Xu, Z.H., and Xue, H.W. (2005). At5PTase13 modulates cotyledon vein development through regulating auxin homeostasis. Plant Physiol. **139:** 1677–1691.

Lou, Y., Gou, J.Y., and Xue, H.W. (2007). PIP5K9, an *Arabidopsis* phosphatidylinositol monophosphate kinase, interacts with a cytosolic invertase to negatively regulate sugar-mediated root growth. Plant Cell **19:** 163–181.

Malamy, J.E., and Benfey, P.N. (1997). Organization and cell differentiation in lateral roots of *Arabidopsis thaliana*. Development **124:** 33–44.

Martin-Belmonte, F., Gassama, A., Datta, A., Yu, W., Rescher, U., Gerke, V., and Mostov, K. (2007). PTEN-mediated apical segregation of phosphoinositides controls epithelial morphogenesis through Cdc42. Cell **128:** 383–397.

Mei, Y., Jia, W.J., Chu, Y.J., and Xue, H.W. (2012). *Arabidopsis* phosphatidylinositol monophosphate 5-kinase 2 is involved in root gravitropism through regulation of polar auxin transport by affecting the cycling of PIN proteins. Cell Res. **22:** 581–597.

Michniewicz, M., et al. (2007). Antagonistic regulation of PIN phosphorylation by PP2A and PINOID directs auxin flux. Cell **130:** 1044–1056.

Mueller-Roeber, B., and Pical, C. (2002). Inositol phospholipid metabolism in *Arabidopsis*: Characterized and putative isoforms of inositol phospholipid kinase and phosphoinositide-specific phospholipase C. Plant Physiol. **130:** 22–46.

Munnik, T. (2014). PI-PLC: Phosphoinositide-phospholipase C in plant signaling. In Phospholipases in Plant Signaling. Signaling and Communication in Plants, Vol. 20, X. Wang, ed (Berlin: Springer-Verlag), pp 27–54.

Munnik, T., and Nielsen, E. (2011). Green light for polyphosphoinositide signals in plants. Curr. Opin. Plant Biol. **14:** 489–497.

Munnik, T., and Testerink, C. (2009). Plant phospholipid signaling: "In a nutshell." J. Lipid Res. **50** (suppl.)**:** S260–S265.

Munnik, T., and Vermeer, J.E. (2010). Osmotic stress-induced phosphoinositide and inositol phosphate signalling in plants. Plant Cell Environ. **33:** 655–669.

Munnik, T., and Zarza, X. (2013). Analyzing plant signaling phospholipids through $^{32}P_i$-labeling and TLC. Methods Mol. Biol. **1009:** 3–15.

Okada, K., Ueda, J., Komaki, M.K., Bell, C.J., and Shimura, Y. (1991). Requirement of the auxin polar transport system in early stages of *Arabidopsis* floral bud formation. Plant Cell **3:** 677–684.

Okushima, Y., et al. (2005). Functional genomic analysis of the AUXIN RESPONSE FACTOR gene family members in *Arabidopsis thaliana*: Unique and overlapping functions of ARF7 and ARF19. Plant Cell **17:** 444–463.

Paciorek, T., Zazímalová, E., Ruthardt, N., Petrásek, J., Stierhof, Y.D., Kleine-Vehn, J., Morris, D.A., Emans, N., Jürgens, G., Geldner, N., and Friml, J. (2005). Auxin inhibits endocytosis and promotes its own efflux from cells. Nature **435:** 1251–1256.

Petrásek, J., et al. (2006). PIN proteins perform a rate-limiting function in cellular auxin efflux. Science **312:** 914–918.

Robert, H.S., Grones, P., Stepanova, A.N., Robles, L.M., Lokerse, A.S., Alonso, J.M., Weijers, D., and Friml, J. (2013). Local auxin sources orient the apical-basal axis in *Arabidopsis* embryos. Curr. Biol. **23:** 2506–2512.

Robert, S., et al. (2010). ABP1 mediates auxin inhibition of clathrin-dependent endocytosis in *Arabidopsis*. Cell **143:** 111–121.

Robles, P., Fleury, D., Candela, H., Cnops, G., Alonso-Peral, M.M., Anami, S., Falcone, A., Caldana, C., Willmitzer, L., Ponce, M.R., Van Lijsebettens, M., and Micol, J.L. (2010). The RON1/FRY1/SAL1 gene is required for leaf morphogenesis and venation patterning in Arabidopsis. Plant Physiol. **152:** 1357–1372.

Sachs, T. (1991). Cell polarity and tissue patterning in plants. Development **1:** 83–93.

Sauer, M., Balla, J., Luschnig, C., Wisniewska, J., Reinöhl, V., Friml, J., and Benková, E. (2006a). Canalization of auxin flow by Aux/IAA-ARF-dependent feedback regulation of PIN polarity. Genes Dev. **20:** 2902–2911.

Sauer, M., Paciorek, T., Benková, E., and Friml, J. (2006b). Immunocytochemical techniques for whole-mount in situ protein localization in plants. Nat. Protoc. **1:** 98–103.

Scarpella, E., Marcos, D., Friml, J., and Berleth, T. (2006). Control of leaf vascular patterning by polar auxin transport. Genes Dev. **20:** 1015–1027.

Simon, M.L., Platre, M.P., Assil, S., van Wijk, R., Chen, W.Y., Chory, J., Dreux, M., Munnik, T., and Jaillais, Y. (2014). A multi-colour/multi-affinity marker set to visualize phosphoinositide dynamics in *Arabidopsis*. Plant J. **77:** 322–337.

Song, S.K., Hofhuis, H., Lee, M.M., and Clark, S.E. (2008). Key divisions in the early *Arabidopsis* embryo require POL and PLL1 phosphatases to establish the root stem cell organizer and vascular axis. Dev. Cell **15:** 98–109.

Sousa, E., Kost, B., and Malhó, R. (2008). *Arabidopsis* phosphatidylinositol-4-monophosphate 5-kinase 4 regulates pollen tube growth and polarity by modulating membrane recycling. Plant Cell **20:** 3050–3064.

Stenzel, I., Ischebeck, T., König, S., Hołubowska, A., Sporysz, M., Hause, B., and Heilmann, I. (2008). The type B phosphatidylinositol-4-phosphate 5-kinase 3 is essential for root hair formation in *Arabidopsis thaliana*. Plant Cell **20:** 124–141.

Stenzel, I., Ischebeck, T., Quint, M., and Heilmann, I. (2012). Variable regions of PI4P 5-kinases direct PtdIns(4,5)P(2) toward alternative regulatory functions in tobacco pollen tubes. Front. Plant Sci. **2:** 114.

Stepanova, A.N., Robertson-Hoyt, J., Yun, J., Benavente, L.M., Xie, D.Y., Dolezal, K., Schlereth, A., Jürgens, G., and Alonso, J.M. (2008). TAA1-mediated auxin biosynthesis is essential for hormone crosstalk and plant development. Cell **133:** 177–191.

Swarup, K., et al. (2008). The auxin influx carrier LAX3 promotes lateral root emergence. Nat. Cell Biol. **10:** 946–954.

Tan, X., Calderon-Villalobos, L.I., Sharon, M., Zheng, C., Robinson, C.V., Estelle, M., and Zheng, N. (2007). Mechanism of auxin perception by the TIR1 ubiquitin ligase. Nature **446:** 640–645.

Tanaka, H., Kitakura, S., Rakusová, H., Uemura, T., Feraru, M.I., De Rycke, R., Robert, S., Kakimoto, T., and Friml, J. (2013). Cell polarity and patterning by PIN trafficking through early endosomal compartments in *Arabidopsis thaliana*. PLoS Genet. **9:** e1003540.

Thole, J.M., Vermeer, J.E., Zhang, Y., and Gadella, T.W., Jr., and Nielsen, E. (2008). Root hair defective4 encodes a phosphatidylinositol-4-phosphate phosphatase required for proper root hair development in *Arabidopsis thaliana*. Plant Cell **20:** 381–395.

Thompson, B.J. (2013). Cell polarity: Models and mechanisms from yeast, worms and flies. Development **140:** 13–21.

Ulmasov, T., Murfett, J., Hagen, G., and Guilfoyle, T.J. (1997). Aux/IAA proteins repress expression of reporter genes containing natural and highly active synthetic auxin response elements. Plant Cell **9:** 1963–1971.

van Leeuwen, W., Vermeer, J.E., and Gadella, T.W., Jr., and Munnik, T. (2007). Visualization of phosphatidylinositol 4,5-bisphosphate in the plasma membrane of suspension-cultured tobacco BY-2 cells and whole *Arabidopsis* seedlings. Plant J. **52:** 1014–1026.

Vanneste, S., and Friml, J. (2009). Auxin: A trigger for change in plant development. Cell **136:** 1005–1016.

Vermeer, J.E., Thole, J.M., Goedhart, J., Nielsen, E., Munnik, T., and Gadella, T.W., Jr., (2009). Imaging phosphatidylinositol 4-phosphate dynamics in living plant cells. Plant J. **57:** 356–372.

Wang, Y., Lin, W.H., Chen, X., and Xue, H.W. (2009). The role of *Arabidopsis* 5PTase13 in root gravitropism through modulation of vesicle trafficking. Cell Res. **19:** 1191–1204.

Weijers, D., Schlereth, A., Ehrismann, J.S., Schwank, G., Kientz, M., and Jürgens, G. (2006). Auxin triggers transient local signaling for cell specification in *Arabidopsis* embryogenesis. Dev. Cell **10:** 265–270.

Wisniewska, J., Xu, J., Seifertová, D., Brewer, P.B., Ruzicka, K., Blilou, I., Rouquié, D., Benková, E., Scheres, B., and Friml, J. (2006). Polar PIN localization directs auxin flow in plants. Science **312:** 883.

Won, C., Shen, X., Mashiguchi, K., Zheng, Z., Dai, X., Cheng, Y., Kasahara, H., Kamiya, Y., Chory, J., and Zhao, Y. (2011). Conversion of tryptophan to indole-3-acetic acid by TRYPTOPHAN AMINOTRANSFERASES OF ARABIDOPSIS and YUCCAs in *Arabidopsis*. Proc. Natl. Acad. Sci. USA **108:** 18518–18523.

Xue, H., Chen, X., and Li, G. (2007). Involvement of phospholipid signaling in plant growth and hormone effects. Curr. Opin. Plant Biol. **10:** 483–489.

Zegzouti, H., Anthony, R.G., Jahchan, N., Bögre, L., and Christensen, S.K. (2006). Phosphorylation and activation of PINOID by the phospholipid signaling kinase 3-phosphoinositide-dependent protein kinase 1 (PDK1) in *Arabidopsis*. Proc. Natl. Acad. Sci. USA **103:** 6404–6409.

Zhang, J., et al (2011). Inositol trisphosphate-induced Ca^{2+} signaling modulates auxin transport and PIN polarity. Dev. Cell **20:** 855–866.

Zhao, Y., Yan, A., Feijó, J.A., Furutani, M., Takenawa, T., Hwang, I., Fu, Y., and Yang, Z. (2010). Phosphoinositides regulate clathrin-dependent endocytosis at the tip of pollen tubes in *Arabidopsis* and tobacco. Plant Cell **22:** 4031–4044.